https://doi.org/10.5194/bg-2021-223
Preprint. Discussion started: 24 August 2021

Biogeosciences Discussions
Open Access
EGU

Modification of methane oxidation pathways during long-term incubations of methanic lake sediments

Hanni Vigderovich[a], Werner Eckert[b], Michal Elul[a], Maxim Rubin-Blum[c], Marcus Elvert[d], Orit Sivan[a]

[a] Department of Earth and Environmental Science, Ben-Gurion University of the Negev, Beer Sheva, Israel
[b] Israel Oceanographic & Limnological Research, The Yigal Allon Kinneret Limnological Laboratory, Migdal, Israel
[c] Israel Limnology and Oceanography Research, Haifa, Israel
[d] MARUM - Center for Marine Environmental Sciences and Faculty of Geosciences, University of Bremen, Bremen, Germany

Corresponding author: Hanni Vigderovich, hannil@post.bgu.ac.il

Abstract

Anaerobic oxidation of methane (AOM) is one of the major processes limiting the release of the greenhouse gas methane from natural environments. In Lake Kinneret sediments, iron-coupled AOM (Fe-AOM) was suggested to play a substantial role (10-15% relative to methanogenesis) in the methanic zone (>20 cm sediment depth), based on geochemical profiles and experiments on fresh sediments. Apparently, the oxidation of methane is mediated by a combination of *mcr* gene bearing archaea and aerobic bacterial methanotrophs. Here we aimed to investigate the survival of this complex microbial interplay under controlled conditions. We followed the AOM process during long-term (~ 18 months) anaerobic slurry experiments of these methanic sediments with two stages of incubations and additions of ^{13}C-labeled methane, multiple electron acceptors and inhibitors. After these incubation stages carbon isotope measurements in the dissolved inorganic pool still showed considerable AOM (3-8% relative to methanogenesis). Specific lipid carbon isotope measurements and metagenomic analyses indicate that after the prolonged incubation aerobic methanotrophic bacteria were no longer involved in the oxidation process, whereas *mcr* gene bearing archaea were most likely responsible for oxidizing the methane. Humic substances and iron oxides are likely electron acceptors to support this oxidation, whereas sulfate, manganese, nitrate, and nitrite did not support the AOM in these methanic sediments. Our results suggest in the natural lake sediments methanotrophic bacteria are responsible for part of the methane oxidation by the reduction of combined micro levels of oxygen and iron oxides in a cryptic cycle, while the rest of the methane is converted by reverse methanogenesis. After long-term incubation, the latter prevails without bacterial methanotropic activity and with a different iron reduction pathway.

Keywords

https://doi.org/10.5194/bg-2021-223
Preprint. Discussion started: 24 August 2021

Anaerobic oxidation of methane (AOM), redox, lake, sediments, dissolved inorganic carbon, stable isotope, electron acceptor

1. Introduction

Methane (CH_4) is an effective greenhouse gas (Wuebbles and Hayhoe, 2002) with anthropogenic and natural origins. Natural methane contributes about 50% of the global methane emissions to the atmosphere (Saunois et al., 2020). Aerobic as well as anaerobic oxidation of methane (AOM) control the release of this greenhouse gas to the atmosphere from its natural sources (Conrad, 2009; Reeburgh, 2007; Knittel and Boetius, 2009). While sulfate-dependent AOM, which is catalyzed by ANaerobic MEthanotrophs ANMEs 1-3, is widespread in marine environments (Hoehler et al., 1994; Boetius et al., 2000; Orphan et al., 2001; Treude et al., 2005, 2014), methane oxidation could theoretically be coupled to other electron acceptors. AOM coupled to reduction of iron and manganese oxides has been experimentally confirmed in several instances (Beal et al., 2009; Egger et al., 2015; Sivan et al., 2011; Sivan et al., 2014; Segarra et al., 2013; Bar-or et al., 2017; Aromokeye et al., 2020; Su et al., 2020). Humic substances, which shuttle electrons in anaerobic environments, may act as the terminal electron acceptors for AOM by ANME-2 (Scheller et al., 2016; Valenzuela et al., 2017; 2019; Bai et al., 2019).

There is also evidence that humic substances and synthetic analogs can stimulate metal-coupled AOM (Bond and Lovley, 2002; He et al., 2019; Valenzuela et al., 2019). Humic substances are considered complex organic compounds rich with redox functional moieties, such as quinones (Scott et al., 1998; Newman and Kolter, 2000; Ratasuk and Nanny, 2007), which provide these substances high redox capabilities (Valenzuela and Cervantes, 2021). The commercial quinone 9,10-anthraquinone-2,6-disulfonate (AQDS) can be used as a terminal electron acceptor (Scheller et al., 2016; Valenzuela et al., 2017; Bai et al., 2019; Zhang et al., 2019; Fan et al., 2020) or an electron shuttle (Lovley et al., 1996; Newman and Kolter, 2000) for AOM. Nitrate dependent AOM have been demonstrated in a consortium of archaea and denitrifying bacteria (Raghoebarsing et al., 2006) and an enrichment culture of ANME-2d (Haroon et al., 2013; Arshad et al., 2015), whereas nitrite fuels AOM by *Methylomirabilis* (NC-10, Ettwig et al., 2010). ANME-2d and *Methylomirabilis* can couple AOM to selenite reduction (Luo et al., 2018). It has also been shown that Methylococcales, which usually require oxygen, may use methane to support denitrification activity under hypoxia (Kits et al., 2015), and may couple methane oxidation and iron reduction (Zheng et al., 2020).

In Lake Kinneret sediments, *in situ* pore water profiles (Sivan et al., 2011), diagenetic modeling (Adler et al., 2011) and incubation experiments with freshly collected sediment slurries (Bar-Or et al., 2017) suggested that iron reduction coupled to AOM (Fe-AOM) removes 10-15% of the produced

https://doi.org/10.5194/bg-2021-223
Preprint. Discussion started: 24 August 2021


Biogeosciences Discussions

methane in the deep methanic zone (>20 cm below water-sediment interface). Analysis of the microbial community structure revealed that both methanogenic archaea and methanotrophic bacteria are potentially involved in the methane oxidation (Bar-Or et al., 2015). Analyses of 16S rRNA amplicons and metagenomics suggested that archaea capable for reverse methanogenesis (probably *Methanothrix* or ANME-1) and the bacterial type I aerobic methanotrophs, Methylococcales, and methylotrophs, *Methylotenera*, play a role in methane cycling (Bar-Or et al., 2017; Elul et al., 2021). The metagenomics analysis together with the isotope enrichment of carbon in bacterial fatty acids following anoxic incubations of the fresh sediment slurries with ^{13}C-labelled methane (Bar-Or et al., 2017), provided evidence for the involvement of Methylococcales in methane oxidation.

This activity of aerobic methanotrophs has been observed in several anoxic lakes' hypolimnions and sediments (Beck et al., 2013; Oswald et al., 2016; Martinez-Cruz et al., 2017; Cabrol et al., 2020), and has been speculated by potential presence of micro levels of oxygen in the deep hypolimnion or sediments, even several meters below the oxycline. Methane oxidation by pure cultures of several different aerobic methanotrophs under hypoxia was attributed to an ability to survive by switching to iron reduction (Zheng et al., 2020) or by self-generation of oxygen by methanobactins (Dershwitz et al., 2021). The latter study also showed the ability of *Methylocystis* sp. Strain SB2, a specific alphaproteobacterial methanotroph, to reduce iron by methane in these unique conditions.

Here, we explored the role of methanotrophic activity in natural methanic lake sediments, its survival outside of the natural conditions during long-term anaerobic incubations, and whether there is a shift in the potential electron acceptors. To answer these questions, we diluted fresh methanic sediments from Lake Kinneret with porewater from the same depth twice and amended the sediment with ^{13}C-labeled methane to follow its oxidation to dissolved inorganic carbon (DIC). These incubations were then also amended with several types of potential electron acceptors and different inhibitors. The results of these experiments were compared to batch and semi-bioreactor experiments that were set up with freshly collected sediments to follow the changes in methane oxidation pathways along the incubation period. We also calculated methane oxidation and production rates of representative pre-incubated long-term slurry experiments. Alongside the ^{13}C-labeled DIC measurements, we investigated the structure of the microbial population using metagenomics and lipid biomarkers to identify the potential microbial players and their dynamics over various incubation periods.

2. Methods

2.1 Study site

Lake Kinneret is a warm monomictic freshwater lake, located in the North of Israel. Its maximum depth is ~42 m and the average depth is 24 m. The lake is thermally stratified from March until December, with the hypolimnion turning anoxic starting from April. The sediment is composed

https://doi.org/10.5194/bg-2021-223
Preprint. Discussion started: 24 August 2021

mostly of carbonates (40-50%) and clays (20%; Hadas and Pinkas, 1995). The total iron content in the top 40 cm of the sediments is ~3 wt % (Serruya, 1971; Eckert, 2000; Bar-Or et al., 2017). The composition of the sediment at the deep methanic depth used in this study (~20 cm sediment depth) was similar with 50% carbonates, 30% clay and 7% iron (Table S1). The dissolved organic carbon (DOC) concentration in the porewater increases with depth, ranging from ~6 mg C L^{-1} at the sediment-water interface to 17 mg C L^{-1} at 25 cm depth (Adler et al., 2011).

2.2 Experimental set-up

This study compares three incubation strategies with Lake Kinneret sediments amended with ^{13}C-labeled methane, different potential electron acceptors for AOM (NO_2^-, NO_3^-, metal oxides and humic substances) and inhibitors for sulfur cycling and methanogens' activity (details below) (Fig. 1):

1) Two stage slurry incubations with 1:1 sediment - pore water ratio for three months, followed by a 1:3 ratio and the addition of different manipulations for up to 18 months.

2) Semi-continuous bioreactor experiments with freshly collected methanic sediments and porewater with 1:4 ratio, where porewater was exchanged regularly.

3) Our previous results gained from batch incubation experiments with freshly collected methanic sediments and porewater with 1:3 ratio and several manipulations (Bar-Or et al., 2017; Elul et al., 2021).

2.2.1 Two stage incubations

The sediments for the slurries were collected between 2017 and 2019 from the central lake (Station A) and pooled from the methanic zone (25 - 40 cm). The sediment was diluted under continuous flushing of N_2 gas with porewater extracted by centrifugation from the same zone to create a 1:1 sediment - pore water ratio slurry (Fig. 1) in 250 ml glass bottles with a headspace of 70-90 ml. The slurries were flushed with N_2 (99.999 %, MAXIMA, Israel) for 30 minutes, after which methane gas was injected to reach 20 % of each bottle headspace, 10 % of the injected methane was ^{13}C-labeled methane (99 %, Sigma-Aldrich) using a gas-tight syringe. After three months of pre-incubation, when ^{13}C-labeled DIC was observed (Fig S1), subsamples (18 g each) were transferred with a syringe under continuous flushing of N_2 gas into 60 ml glass bottles and diluted with fresh anaerobic porewater to achieve a 1:3 sediment - pore water ratio (Fig. 1), which leaves 24 ml of headspace in each experiment bottle. All pre-incubated experiment bottles were crimp-sealed, flushed with N_2 gas for 5 minutes, shaken vigorously and flushed again (3 times).

To verify the role of different potential electron acceptor/s and inhibitors we conducted ten experiments as outlined in Table S2. The possible influence of sulfate reduction and sulfur disproportionation on AOM was investigated by adding Na-molybdate (Lovley and Klug, 1983), to an

https://doi.org/10.5194/bg-2021-223
Preprint. Discussion started: 24 August 2021


Biogeosciences Discussions

already running experiment in case of an active cryptic sulfur cycle, even with the absence of detectable sulfate (Holmkvist et al., 2011). Other inhibitors added were 2-bromoethanesulfonate (BES, Nollet et al., 1997) and acetylene (Oremland and Capone, 1988) (Table S2). BES is a specific inhibitor for methanogens and ANME's *mcrA* genes, and acetylene is a non-specific inhibitor for methanogens (among others, as discussed later). BES was added at the beginning of the experiment, while acetylene gas was injected during the experiment to two bottles at different timepoints. Electron acceptors were added either as powder (hematite, magnetite, clay, MnO_2, humic substances) or in dissolved form (KNO_3 and $NaNO_2$). AQDS and phenazine-1-carboxylate (PCA) were dissolved in double distilled water (DDW) and then added. Amorphic iron ($Fe(OH)_3$) was prepared in the lab, by dissolving $FeCl_3$ in DDW, which was then titrated with NaOH 1.5 N, until the solution reached pH 7. The $Fe(OH)_3$ was added to the bottles by injection. The final concentration of each addition is described in table S2. The ^{13}C-labeled methane was injected into all experiment bottles using a gas-tight syringe from a stock bottle filled with ^{13}C-labeled methane gas (which was replaced with saturated NaCl solution). Electron acceptors and ^{13}C-labeled methane were added to the "killed" control bottles after they were autoclaved twice and cooled. The variations in the $\delta^{13}C_{DIC}$ values between the experiments are the result of different amounts of ^{13}C-labeled methane injected at the start of each experiment. 2 ml of porewater were sampled anaerobically for $\delta^{13}C_{DIC}$ (duplicates were taken from each experimental bottle) and dissolved Fe(II) concentrations during each sampling point from all experimental bottles. Methane was measured from the headspace (duplicates from each experimental bottle) and the porewater concentrations were calculated using the volume of the bottles and the slurries. All live treatments were set up in duplicates or triplicates, except for the black coffee treatment, which only had one replicate as an attempt to check a close analog for humic substances. In 4 experiments only one "killed" control bottle was set up because these controls had been showing repetitive results (no activity) for numerous previous experiments. For the humic substrate experiment we received natural humic substance extracted from a lake by a colleague in the University of Alaska, Fairbanks. One experiment was set up without any additional electron acceptor in order to assess the rate of methanogenesis in the pre-incubated slurries.

2.2.2 Semi-bioreactor experiment

Two semi-bioreactors (Fig. 1) were set up with fresh sediments from the methanic zone (25 - 40 cm) of Lake Kinneret central station (Station A) immediately after their collection. Both reactors were filled headspace-free with a slurry of a 1:4 sediment - pore water ratio. One of the bioreactors was amended with 10 mM hematite. To dissolve ^{13}C-labeled methane in the porewater, 15 ml of headspace was produced with only methane gas for 24 hours. The reactors were shaken repeatedly during those hours. After 24 hours, the gas was replaced with anoxic pore-water, so that there was no head-space at all. The oxidation-reduction potential was monitored continuously by a redox electrode (Metrohm, Herisau, Switzerland) throughout the incubation period to verify anoxic conditions and to

https://doi.org/10.5194/bg-2021-223
Preprint. Discussion started: 24 August 2021

know the redox state of the slurry in the reactor. The bioreactors were subsampled weekly to bi-weekly, and the sample volume (5-10 ml) was replaced immediately by preconditioned anoxic (flushed with N_2 gas for 15 minutes before the exchange) porewater from the methanic zone. Samples were analyzed for dissolved Fe(II), CH_4 and $\delta^{13}C_{DIC}$ as outlined below. Additional subsamples for metagenome analysis and lipid analysis were taken at the beginning of the experiment and on day 151, and day 382 respectively. The purpose of the semi-bioreactors was to set up an experiment that can monitor the redox state regularly, to have a closer to natural conditions, and to have another indication for the processes involving methane in freshly collected sediments.

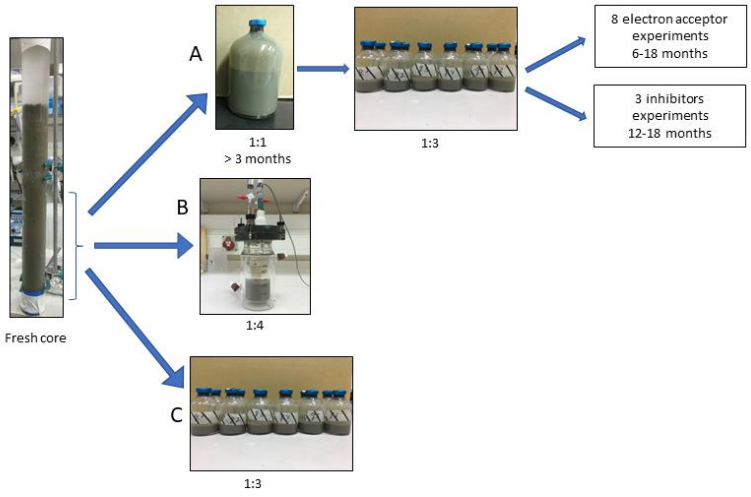

Figure 1: Flow diagram of experimental design. Three types of experiments were set up from sediments of the deep methanic zone (below 25 cm): A. Pre-incubated slurry experiments. Fresh sediments collected from the lake were incubated in a 1:1 ratio with porewater extracted from the same depth for 3 months. Then the slurry was divided to the experiments bottles and diluted again with fresh porewater to reach 1:3 ratio. 10 experiments were set up this way, 8 of them with different electron acceptors for 6-18 months, and 3 with different inhibitors for 12-18 months (to one experiment both electron acceptor and an inhibitor were added). B. Semi-bioreactor experiment. Fresh sediments collected from the lake were inserted to two bioreactors and diluted with fresh porewater to reach 1:4 ratio. The bioreactors were set up with no headspace. One of the bioreactors was amended with iron oxide (hematite). C. Slurry experiment with freshly collected sediments. The sediments were diluted with porewater to reach 1:3 ratio, and was amended with different iron oxides (Bar-Or et al., 2017). The experiment was set up for 17 months.

2.3 Porewater analyses

About 0.3 ml of filtered (0.22 um) pore-water was injected to 12 ml glass vial with He atmosphere and 10 µl of H_3PO_4 85% to acidify all the DIC species to CO_2 (g). The autosampler takes a gas sample from the vials and measures the $\delta^{13}C_{DIC}$ of the sample on the GasBench interface of a DeltaV Advantage Thermo Scientific isotope-ratio mass-spectrometer (IRMS) at a precision of ±0.1 ‰. It should be noted that to measure $\delta^{13}C_{CH4}$ the gas sample must be combusted before this procedure, which means that the $\delta^{13}C$ measured is of the DIC only. Results are reported versus the Vienna Pee

https://doi.org/10.5194/bg-2021-223
Preprint. Discussion started: 24 August 2021


Biogeosciences Discussions

Dee Belemnite (VPDB) standard. Dissolved Fe(II) concentrations were measured using the ferrozine method (Stookey, 1970) by a spectrophotometer at 562 nm wavelength with a detection limit of 1 µmol L^{-1}. A gas sample was taken from the experiment bottle's headspace by a gas-tight syringe and was analyzed for methane and ethylene concentrations by a focus gas chromatograph (GC) equipped with a flame ionization detector (FID) with a detection limit of 50 µmol L^{-1}. Methanogenesis rate was derived from temporal changes in methane concentration in a representative pre-incubated slurry experiment (Fig. S2). The amount of methane oxidized was calculated by a simple mass balance calculation according to Eq. 1 and 2:

$$x \times F^{13}CH_4 + (1 - x) \times FDI^{13}C_i = FDI^{13}C_f \quad (1)$$

$$[CH_4]_{ox} = x \times [DIC]_f \quad (2)$$

Where x is the mixing fraction of two sources which compose the final DIC; the initial DIC pool and the oxidized ^{13}C-CH_4. The letter x denotes the fraction of oxidized ^{13}C-CH_4, while 1-x denotes the fraction of the initial DIC pool out of the final DIC pool. $F^{13}CH_4$ is the fraction of ^{13}C out of the total CH_4 at t0, $FDI^{13}C_i$ is the fraction of ^{13}C out of the total DIC at t0, and $FDI^{13}C_f$ is the fraction of ^{13}C out of the total DIC at t-final. $[CH_4]_{ox}$ is the amount (concentration in pore water) of the methane oxidized throughout the full incubation period, and $[DIC]_f$ is the DIC concentration at t-final. We assumed that the isotopic composition of the labeled CH_4 did not change significantly throughout the incubation period.

2.4 Lipid analyses

A sub-set of samples was investigated for the assimilation of ^{13}C-labeled methane into polar lipid-derived fatty acids (PLFAs) and intact ether lipid-derived hydrocarbons. A total lipid extract (TLE) was obtained using a modified Bligh and Dyer protocol (Sturt et al., 2004). PLFAs in the TLE were converted to fatty acid methyl esters (FAMEs) using saponification with KOH/MeOH and derivatization with BF_3/MeOH (Elvert et al., 2003). Intact archaeal ether lipids in the TLE were separated from the apolar archaeal lipid compounds using preparative liquid chromatography (Meador et al., 2014) followed by ether cleavage with BBr_3 in dichloromethane forming hydrocarbons (Lin et al., 2010). Both FAMEs and ether-cleaved hydrocarbons were analyzed by GC-mass spectrometry (GC-MS; Thermo Finnigan Trace GC coupled to a Trace MS) for identification and GC-IRMS (Thermo Scientific Trace GC coupled via a GC Isolink interface to a Delta V Plus) for the determination of $\delta^{13}C$ values using the column and temperature program settings described by Aepfler et al. (2019) . $\delta^{13}C$ values are reported with an analytical precision better than 1 ‰ as determined by long-term measurements of an *n*-alkane standard with known isotopic composition of each compound. Reported fatty acid isotope data are corrected for the introduction of the methyl group during

https://doi.org/10.5194/bg-2021-223
Preprint. Discussion started: 24 August 2021

derivatization by mass balance calculation similar to eq. 1 using the measured $\delta^{13}C$ value of each FAME and the known isotopic composition of methanol as input parameters.

2.5 Metagenome analysis

Total genomic DNA was extracted from the semi-bioreactor experiment (duplicates a and b), pre-incubation 1:1 experiments ($^{13}CH_4$-only control, $^{13}CH_4$ + hematite) and their respective initial slurries (t0), using the DNeasy PowerLyzer PowerSoil Kit (QIAGEN). Genomic DNA was eluted using 50 µl of elution buffer and stored at −20°C. Metagenomics libraries were prepared at the sequencing core facility at the University of Illinois at Chicago using Nextera XT DNA library preparation kit (Illumina, USA). 19-40 million 2 × 150 bp paired-end reads per library were sequenced using Illumina NextSeq500. For each library, taxonomic diversity was determined by mapping the reads to Silva V138.1 database of the small subunit rRNA sequences using phyloFlash (Glöckner et al., 2017; Gruber-Vodicka et al., 2019). Metagenomes were co-assembled from concatenated reads of all metagenomic libraries with Spades V3.12 (Bankevich et al., 2012; Nurk et al., 2013), following decontamination, quality filtering (QV= 10) and adapter-trimming with the BBDuk tool from the BBMap suite (Bushnell B, http://sourceforge.net/projects/bbmap/). Downstream analyses, including read coverage estimates, automatic binning with maxbin (Wu et al., 2014) and metabat2 (Kang et al., 2019) bin refining with DAS tool (Sieber et al., 2018), were performed within the SqueezeMeta framework (Tamames and Puente-Sánchez, 2019).

3. Results

In this study we followed the progress of the methane oxidation process in long-term incubations from Lake Kinneret methanic sediments. This is by quantifying the modifications between experiments conducted on fresh sediments from the methanic zone (batch slurries presented by Bar-Or et al. (2017) and Elul et al. (2021) and semi-bioreactor slurries) and pre-incubated long-term batch slurry experiments.

3.1 Geochemical trends

In the pre-incubated long-term experiments, similarly to the fresh incubations, there was a conversion of ^{13}C-methane to ^{13}C-DIC in all the natural non-killed slurries, indicating significant AOM (Figs. 2-3). The $\delta^{13}C_{DIC}$ values in the natural slurries (so called methane-only control) reached hundreds of permilles, even with the low abundance of microbial populations in these sediments (Elul et al., 2021).

The geochemical experiments tested the potential of several electron acceptors to perform and stimulate this considerable AOM process. It should be noted that the actual involvement of sulfur cycling can be quantified directly by inhibiting this cycle, while the rest can be tested for their

https://doi.org/10.5194/bg-2021-223
Preprint. Discussion started: 24 August 2021


Biogeosciences Discussions

263 potential involvement by their addition to the slurries. First, metal oxides were added. The addition of
264 hematite as an electron acceptor did not change the $\delta^{13}C_{DIC}$ increase with time (the slope) compared to
265 the methane-only controls (Fig. 2). This is in contrast with the freshly collected sediment experiments,
266 where this addition stimulated the conversion of ^{13}C-methane to ^{13}C-DIC and thus the AOM (Fig. 2).
267 Magnetite amendments resulted in less increase in $\delta^{13}C_{DIC}$ values as compared to the methane-only
268 controls (to 290‰ and ~360‰, respectively, Fig. 3A), and amorphous iron amendments showed even
269 lower values (Fig. 3A). The addition of nontronite (iron bearing clay) did not cause any increase in the
270 $\delta^{13}C_{DIC}$ values, however, it did result in an increase in the dissolved Fe(II) concentrations compared to
271 the natural control (Fig. 3F, Fig. S3). The $\delta^{13}C_{DIC}$ values of the bottles with the addition of MnO_2 also
272 did not show any indication for AOM after 200 days, whereas the $\delta^{13}C_{DIC}$ values of the methane-only
273 controls reached over 500‰ (Fig. 3B).

274 The actual involvement of sulfate was quantified directly by the addition of Na-molybdate, an
275 inhibitor of sulfate reduction and sulfur disproportionation, to the methane-only controls and to
276 slurries amended with magnetite (Fig. 3A). This addition did not change the slope of the $\delta^{13}C_{DIC}$
277 increase with time, clearly indicating no AOM inhibition and no role for sulfate in the AOM process.
278 Nitrate was added in two different concentrations (0.2 and 1 mM Fig. 3C) to the long-term slurries
279 amended with hematite, as these concentrations were shown previously to promote AOM in other
280 settings (Ettwig et al., 2010). Hematite addition alone increased the $\delta^{13}C_{DIC}$ values by circa 200‰
281 during 306 days of the experiment. The $\delta^{13}C_{DIC}$ in the bottles with the addition of 1 mM of nitrate,
282 with and without hematite, decreased on the other hand from 43‰ at the beginning of the experiment
283 to 35‰ after 306 days. The $\delta^{13}C_{DIC}$ in the bottles with the addition of 0.2 mM nitrate and hematite
284 increased only slightly in the end. We also observed no increase in $\delta^{13}C_{DIC}$ during the first 222 days
285 following the addition of 0.5 mM of nitrite (Fig. 3D), while $\delta^{13}C_{DIC}$ increased by 19‰ afterward until
286 the incubation was terminated. Following the addition of 0.1 mM nitrite, $\delta^{13}C_{DIC}$ increased only after
287 130 days and reached 158‰ at day 493. In the methane-only controls, $\delta^{13}C_{DIC}$ values reached the
288 highest values (330‰).

289 We also amended long-term pre-incubated slurries with potential organic electron acceptors. No
290 $^{13}C_{DIC}$ enrichment was observed with the addition of AQDS (an analog for humic substrate) to slurries
291 with and without hematite (Fig. 3E). Similar trends were observed in $\delta^{13}C_{DIC}$ following the addition of
292 PCA, an analog for methanophenazines that are found in some archaeal membranes and shuttle
293 electrons (Wang and Newman, 2008) (Fig. 3F). We further tested the effect of naturally occurring
294 humic substances, using those isolated from a different natural lake. The results show that in the
295 beginning the $\delta^{13}C_{DIC}$ values did not change (Fig. 3F), while a steep increase in their Fe(II)
296 concentrations was observed (Fig. S3). However, after 20 days, the $\delta^{13}C_{DIC}$ values of these slurries
297 started to increase dramatically with a steep slope, indicating high AOM activity (Fig. 3F). We also

https://doi.org/10.5194/bg-2021-223
Preprint. Discussion started: 24 August 2021

298 tested the addition of black coffee, as another example of a complex natural organic substance. In this
299 incubation, again, the $\delta^{13}C_{DIC}$ values decreased during the first 20 days, but then increased very
300 steeply (from 102‰ to 596‰). In those additions there is in general a mirrored trend of the dissolved
301 Fe(II) concentrations to that of $\delta^{13}C_{DIC}$ with a steep increase, from 65 to 170 µM, during the first 20
302 days
303 and
304 then
305 a

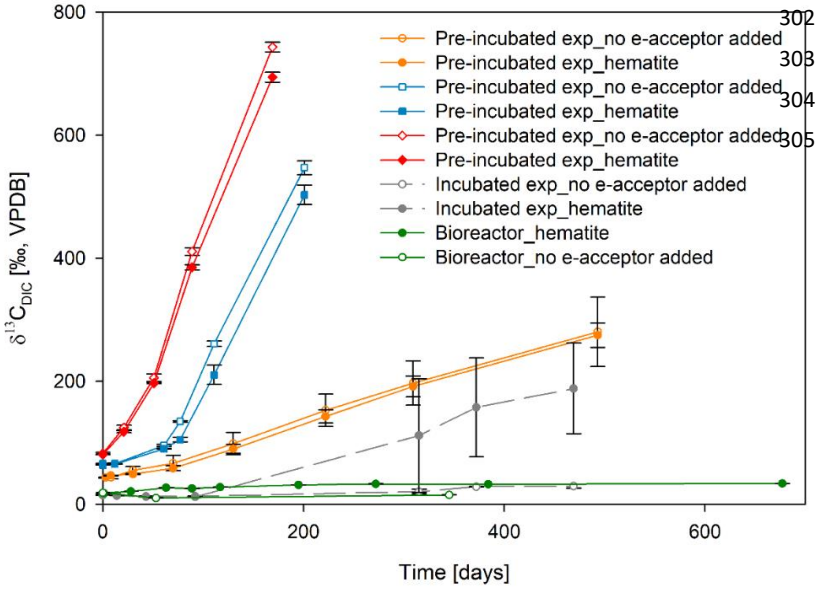

Figure 2: Comparison of $\delta^{13}C_{DIC}$ values between the three types of experiments: three pre-incubated long-term slurry experiments (pre-incubated exp), the bioreactor experiment, and a slurry experiment with freshly collected sediments (incubated exp, (Bar-Or et al., 2017)). In each experiment, two treatments are shown - with hematite (filled symbol) and without (empty symbols) hematite addition. The error bars represent the average deviation of the mean of duplicates/triplicates bottles.

306 decrease (from 170 µM to 133 µM, Fig. S3).

307 Geochemical analysis of $\delta^{13}C_{DIC}$ was performed also on two experiments that tested the effect of
308 inhibitors on methane metabolism. In one experiment, BES, a specific inhibitor for methanogens and
309 ANME's *mcrA* genes, was added, and in another experiment, acetylene, a non-specific inhibitor for
310 methanogens, was added. Both cases showed a complete inhibition of labeled ^{13}C-DIC production
311 following the addition, similarly to the killed control (Fig. 4). Acetylene can also inhibit nitrogen
312 cycling in some cases, however ethylene is produced then (Oremland and Capone, 1988). In our case
313 no ethylene was detected, supporting the inhibition only of methanogens' activity.

314

https://doi.org/10.5194/bg-2021-223
Preprint. Discussion started: 24 August 2021

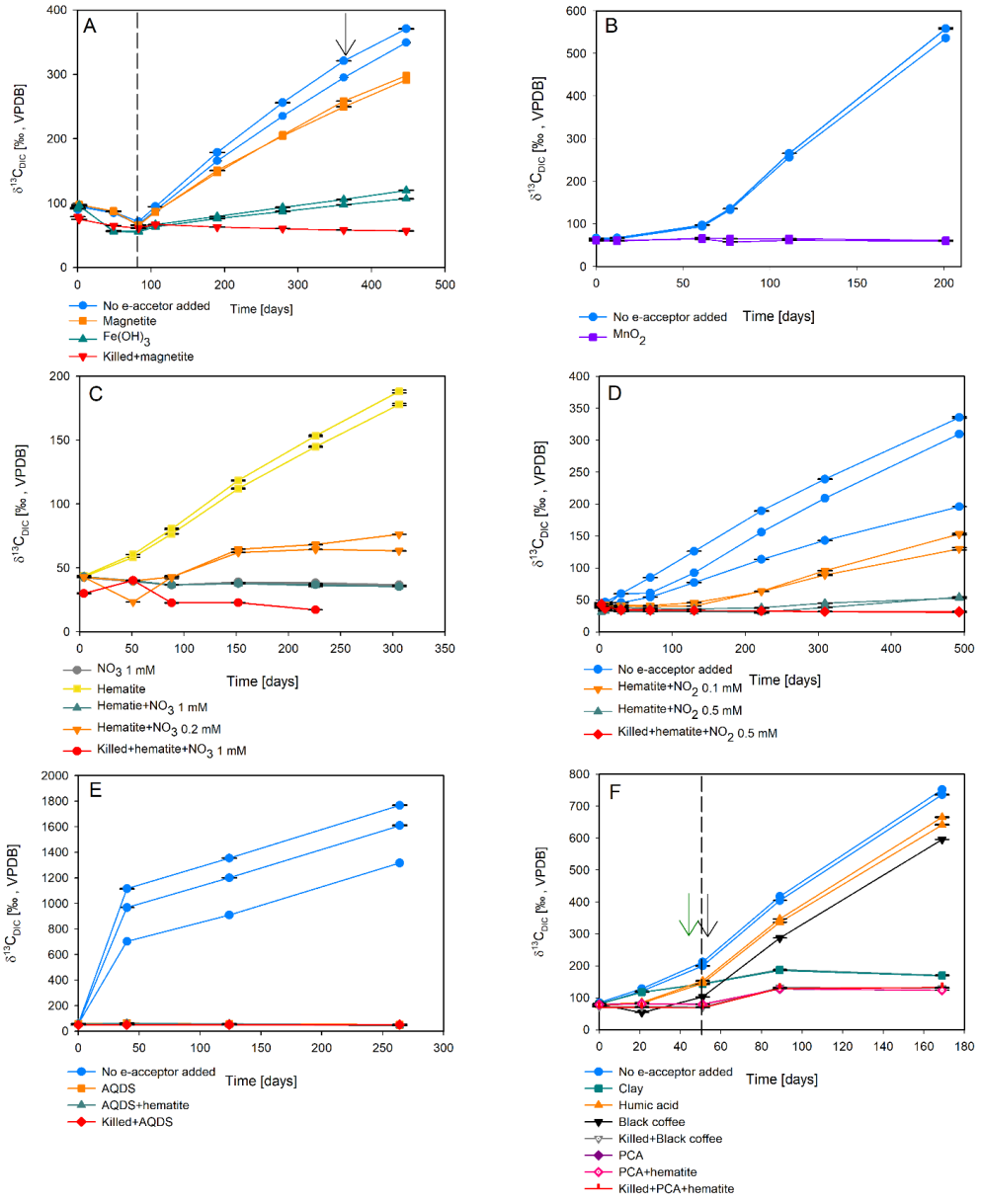

315 Figure 3: The potential of different electron acceptors for AOM in Lake Kinneret sediments. In these pre-incubated long-term slurry experiments, the following treatments have been applied: (A) with and without the addition of magnetite and amorphous iron ($Fe(OH)_3$). Dashed line represents addition of ^{13}C -labeled CH_4. Back arrow represents addition of sodium molybdate as an inhibitor for sulfate reduction. (B) with and without the addition of MnO_2. (C) with the addition of hematite and two different concentrations of nitrate. (D) with the addition of hematite and two different concentrations of nitrite. (E) with the addition of AQDS. (F) with clay, natural humic acid, black coffee and PCA. Green arrow represents the time clay was added to the relevant bottles, the dashed line represents the time the headspace of the bottles was flushed again with N_2, and the black arrow represents the second injection of 1 mL of ^{13}C -labeled methane. ^{13}C -labeled methane was added to all the bottles (specific details on each experiment can be found in Table S2). Each data point is the average of duplicate samples that were taken from each bottle; the error bars are smaller than the symbol.

https://doi.org/10.5194/bg-2021-223
Preprint. Discussion started: 24 August 2021

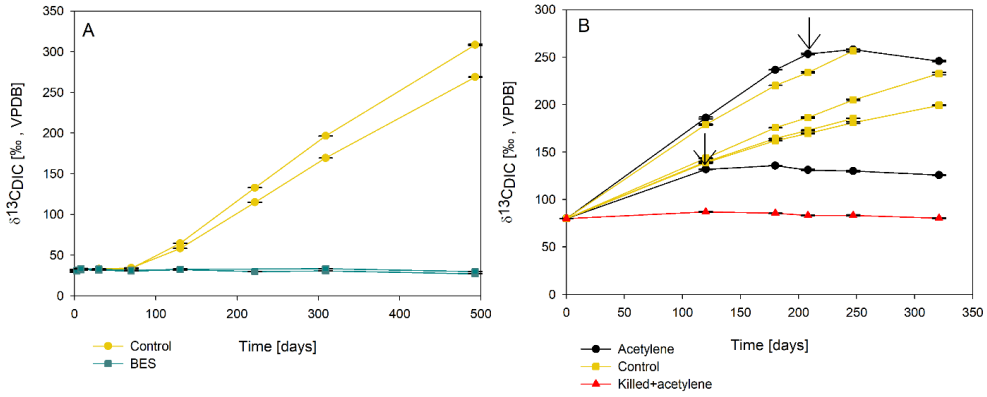

Figure 4: The change of $\delta^{13}C_{DIC}$ values with time in two long-term sediment slurry incubations amended with hematite and ^{13}C-labeled methane. (A) with/out BES and (B) with/out acetylene. Black arrows represent the time point where acetylene was injected to the experiment bottle. The error bars are smaller than the symbols.

3.2 Metagenomic and lipid analyses

The metagenomic analysis points to the potential involvement of several archaea and bacteria in the AOM observed in the pre-incubated slurries. Bona fide ANME (ANME-1), as well as various methanogens and high abundance of Bathyarchaeia were present in all the samples (Table S3). Known sulfate reducing bacteria, including Desulfobacterota, Desulfuromonadota and Thermodesulfovibrionia, but not seep sulfate reducing bacteria, were found, and some in large read abundances (Table S3). Only very few metagenomic reads mapped to Methylomirabilaceae (NC-10) (<1%) and no reads mapped to *Methanoperedens*. The number of metagenomic reads mapped to functional genes *narH* and *narG*, which encode subunits of the respiratory nitrate reductase in *Methanoperedens* decreased with time in the pre-incubated sediments (Table S4). Very few reads mapped to the *nirS* gene, which encodes the nitrite reductase, and its coverage did not increase over time (Table S4).

The $\delta^{13}C$ values of the archaeol-derived isoprenoid phytane showed ^{13}C-enrichment (between 15-27‰ enrichment), and no ^{13}C-enrichment in the killed control, indicative of methane assimilation by archaea. This signal was also found for acyclic biphytane but less pronounced (between 5-10‰ enrichment) (Table 1).

https://doi.org/10.5194/bg-2021-223
Preprint. Discussion started: 24 August 2021

Biogeosciences Discussions Open Access EGU

Table 1: $\delta^{13}C$ values (in ‰) of fatty acids and isoprenoid hydrocarbons from different 1:1 incubations and experiments compared to values obtained from the original sediment in the methanic zone.

			Fatty acids		Hydrocarbons	
Description	Temperature (°C)	Sampling (days)	$C_{16:1\omega9/8/7}$	$C_{16:1\omega5}$	Phytane	Biphytane
Incubated bottle +$^{13}CH_4$+hematite	20	411	-40	-43	-17	-23
Incubated bottle +$^{13}CH_4$	20	411	-40	-43	-13	-24
Incubated bottle +$^{13}CH_4$	20	1227	-36	-41	-5	-38
[a]Typical fresh sediment incubated bottle hematite+$^{13}CH_4$	20	470	610	1600	-14	-28
Bioreactor+$^{13}CH_4$+hematite	16	382	n.d.	n.d.	n.d.	n.d.
Original sediment (28-30 cm)	14		-44	-50.7	-32	-33

[a] Bar-Or et al., 2017
n.d. – Not detected

4. Discussion

Our many porewater profiles of Lake Kinneret indicate that microbial sulfate reduction dominates the anoxic hypolimnion and the surface sediments, while methanogenesis is confined to the sediments below the sulfate boundary (Adler et al., 2011; Sivan et al., 2011; Bar-Or et al., 2015; Elul et al., 2021). Our previous work on fresh sediments from the lake also provided evidence for Fe-AOM in the methanic zone based mainly on geochemical and microbiological profiles and models (Adler et al., 2011; Sivan et al., 2011; Bar-Or et al., 2015). It was combined also with measurements of stable carbon isotopes in specific lipids and microbial metagenomic analyses during ^{13}C-labeled methane batch incubations on fresh sediments from the methanic zone (Bar-Or et al., 2017; Elul et al., 2021; Fig. 2). These showed the unexpected significant abundance of known aerobic bacterial methanotrophs together with anaerobic microorganisms (as methanogens and iron reducers).

The first noticeable observation from the current pre-incubated long-term slurries data is that the $\delta^{13}C_{DIC}$ values of the natural amendments (only with the addition ^{13}C-labeled methane) increased dramatically. This indicates a clear AOM signal, even after the long-term incubations and the low abundance of the microbial populations. Below, we characterize this AOM process.

4.1 Potential electron acceptors for AOM in the long-term pre-incubated experiments

The pre-incubated long-term incubations data show a sharp increase in the $\delta^{13}C_{DIC}$ values of both natural and hematite amendments. However, as opposed to the freshly collected sediment experiments, there was no difference between the addition of hematite as the electron acceptor and the natural (methane-only) amendment. This means that hematite does not have a potential to stimulate the AOM activity or that there is enough natural Fe(III) in the sediments to sustain the maximum potential of Fe-AOM.

https://doi.org/10.5194/bg-2021-223
Preprint. Discussion started: 24 August 2021

Following this observation, we quantified the effect of other metal oxides, such as magnetite, amorphous iron, and manganese oxide (Fig. 3A and B), which are present in Lake Kinneret sediments (Bar-or et al., 2017), on AOM in the long-term incubation slurries from the methanic zone. The results show that the addition of any of these iron oxides showed less increase in the $\delta^{13}C_{DIC}$ values compared to the methane only controls (Figs. 2 and 3). This indicates not only that their addition did not stimulate AOM it might even inhibit it. The less increase in the $\delta^{13}C_{DIC}$ values with their addition could result from their direct inhibition of the AOM process or by their reduction by organic compounds other than methane (organoclastic iron reduction), which added isotopically light carbon from the organics and not heavy carbon from the ^{13}C-labeled methane (masking the natural AOM signal shown in the natural control). We further tested whether ferric iron from clays, which can act as terminal electron acceptors (Kostka et al., 2002; Liu et al., 2011; Liu et al., 2012), could support AOM. However, the addition of the clay minerals appears again to encourage only organoclastic iron reduction (Fig. 3F, Fig. S3). Like iron oxides, manganese oxide, did not support AOM and likely encouraged organoclastic manganese reduction. Given that manganese oxides are found in very low abundance in Lake Kinneret sediments (0.1 %, Table S1), their potential role in metal-AOM is likely low anyway.

Sulfate concentrations in the methanic Lake Kinneret sediments are low (< 5 µM, Bar-Or et al., 2015; Elul et al., 2021). Sulfide concentrations are accordingly minor (<0.3 µM, Sivan et al., 2011). However, since pyrite and FeS precipitate in the top sediments, cryptic cycling via pyrite or FeS may replenish sulfate accessible for AOM (Bottrell et al., 2000). The role of sulfate as an electron acceptor was tested directly by the addition of Na-molybdate as an inhibitor for sulfate reduction. This addition to the long-term pre-incubated slurries amended with and without magnetite (Fig. 3A) did not change the $\delta^{13}C_{DIC}$ values, and they increased similar to the natural (methane only) control, as occurred also in the fresh batch sediment slurries (Bar-Or et al., 2017). This indicate clearly that sulfate is not involved in the AOM process in Lake Kinneret methanic sediments, as the inhibition of the sulfur cycling did not inhibit the AOM. This is despite the presence of potential sulfate-reducing bacteria as indicated by their relatively high abundance (Table S3) in the sediments.

The concentrations of both, nitrate and nitrite, are also below detection in the porewater of Lake Kinneret sediments (Nüsslein et al., 2001), but their occurrence as an intermediate product through ammonium oxidation coupled to iron reduction (Li et al., 2015; Shuai and Jaffé, 2019) cannot be excluded. Therefore, the potential role of nitrate and nitrite as electron acceptors in the pre-incubated slurries was quantified. The results indicate that rather than stimulating AOM, the addition of nitrate (Fig. 3C) delayed AOM and promoted organoclastic denitrification. Similarly, even low nitrite concentrations appeared to inhibit AOM, potentially facilitating denitrification (Fig. 3D).

https://doi.org/10.5194/bg-2021-223
Preprint. Discussion started: 24 August 2021

Humic substances were also investigated as potential electron acceptors for the AOM process. They could also promote AOM by continuously shuttling electrons to metal oxides (Valenzuela et al., 2019). Humic substances were not measured specifically in Lake Kinneret sediments, but DOC concentrations in the pore-water at the methanic depth were high (~1.5 mM, Adler et al., 2011), suggesting their possible role in the AOM process. The addition of the synthetic humic analogs AQDS did not cause any enrichment in ^{13}C of the DIC. This could be due to their high electron shuttling ability and encouraging organoclastic oxidation that adds light carbon isotope (as opposed to the labeled ^{13}C-methane) and lowers the $\delta^{13}C_{DIC}$ values without AOM at all, or by masking its signal (Fig. 3E). Similar trends were observed in $\delta^{13}C_{DIC}$ following the addition of PCA, a synthetic analog for methanophenazines (Fig. 3F). Yet, the addition of natural humic acids or black coffee exhibited different behavior. At first, the natural humic substances promoted organoclastic iron reduction, probably by shuttling electrons from organic compounds other than methane to natural iron oxides in the sediments (Figs. 3F, S3). Then, perhaps when the availability of the iron oxides or the organic matter decreased, humic substances were used as terminal electron acceptors for AOM, as was suggested by Valenzuela et al. (2017). In that study, AOM was coupled to the reduction of humic substances in the presence of inorganic electron acceptors simultaneously with methanogenesis.

Overall, our experiments with different electron acceptors indicate clearly that sulfate is not involved in the AOM process in Lake Kinneret methanic sediments, and that nitrate, nitrite and Mn-oxides are less likely. The potential electron acceptors are natural humic substrates with or without iron minerals that are abundant in the sediment and preferably react with methane rather than with other organics.

4.2 Main microbial players in the long-term pre-incubated experiments

As mentioned above, the pre-incubated long-term incubations data show a sharp increase in the $\delta^{13}C_{DIC}$ values of natural amendments. However, the addition of BES, a specific inhibitor for methanogens and ANME's *mcrA* genes, stopped immediately the AOM, similarly to the killed bottles, and to the fresh sediment experiments (Bar-Or et a., 2017), indicating methane oxidation by methanogens or ANMEs in all stages of incubations (Fig. 3). In addition, the complete inhibition of labeled DIC production following the addition of acetylene (Fig. 4) suggests the involvement of methane metabolizing microorganisms, also evidenced by the enrichment in $\delta^{13}C$ values of phytane and biphytane (Table 1). Such a signal is generally indicative of active archaea, i.e. methanogens or ANMEs in this case, which assimilate ^{13}C-carbon from an unknown intermediate or existing DIC.

The essential role of methanogens or ANMEs in the AOM in all stages of incubations suggest that this process is performed by reverse methanogenesis. Indeed, in metagenome-assembled genomes (MAGs) of ANME-1 and *Methanothrix*, all the seven genes (*mcr, mtr, mer, mtd, mch, ftr, fmd*) needed for the reverse methanogenesis (Meyerdierks et al., 2010; Wang et al., 2014; Wegener et al., 2021) were found. It should be noted that ANME-1 was found in very low abundance (< 1.5 %) and other

https://doi.org/10.5194/bg-2021-223
Preprint. Discussion started: 24 August 2021

ANMEs were not found at all. In addition, while the abundant Bathyarchaeia in all incubation stages might be involved in methane metabolism (Evens et al., 2015), the *mcrA* genes were not found in their Lake Kinneret MAGs, thus their role in AOM is questionable.

On the other hand, both the metagenomic and lipid isotopic analysis suggest that the role of aerobic type I methanotrophs (of the class gammaproteobacteria) in methane turnover in the long-term incubations is negligible (Table S3). This contrasts with the natural sediments and fresh incubations that show their presence in the sediments and their important role in oxidizing the methane.

4.3 Methane oxidation pathway in the long-term incubations

Our results indicate net methanogenesis in long-term incubations with an average rate of 2 μM day^{-1} (Fig. S2 and Table S5), similarly to the fresh incubation experiments (Bar-Or et al., 2017). This is even with the overall development of increasing $\delta^{13}C_{DIC}$ values resulting from potential methane turnover (Fig. 2 and 3). A likely explanation for this signal is an interplay between methane production and oxidation, with the latter triggered by reverse methanogenesis, which is demonstrated among the orders of methanogens and ANMEs (Hallam et al., 2004; Timmers et al., 2017). Of these, *Methanothrix* (closely related to the order Methanosarcinales) has high potential to perform reverse methanogenesis here and in other environmental settings (Valenzuela et al., 2017; 2019; Elul et al., 2021). In our sediments, Methanosarcinales were also found to increase in abundance towards the methanic zone (Bar-Or et al., 2015). Reverse methanogenesis is used in trace methane oxidation by pure cultures of various species of the *Methanosarcina* and the *Methanbacterium* genera (Zehnder and Brock, 1979; Moran et al., 2005, 2007; Luo et al., 2017; Lai et al. 2018).

Due to the overall production of methane and the lack of intensive stimulation of AOM by any electron acceptor, the high increase in $\delta^{13}C_{DIC}$ could also theoretically result from carbon back flux during methanogenesis, which is feasible in environments close to thermodynamic equilibrium (Gropp et al., 2021). To determine whether back flux is feasible in the incubations, we assessed how much of methane is oxidized and converted to DIC using mass balance calculations. To reach the observed ^{13}C-enrichment in our experiments, 3-8 % of the ^{13}C-methane had to be channeled into DIC through Eq. 1 and 2, which is much higher than the previously reported methanogenesis back flux values (0.3-0.001 %, Zehnder and Brock, 1979; Moran et al., 2005). Back flux reactions have been studied before only in ANME-enrichment cultures and by modeling approaches in marine environments without indications of net methanogenesis (Holler et al., 2011; Yoshinaga et al., 2014; Chuang et al., 2019; Meister et al., 2019; Wegener et al., 2021). During net AOM conditions, however, this process was recently attributed to intracellular reversibility of enzymes involved in the reaction chain under substrate limitation without invoking methane-DIC equilibration (Wegener et al., 2021). Indeed, low methanogenesis rates in the environment may result in enhanced back flux, compared to the active methanogenic cultures (Hoehler et al., 1994; Holler et al., 2011). Yet, based on

https://doi.org/10.5194/bg-2021-223
Preprint. Discussion started: 24 August 2021

the above, it is unlikely that back flux alone will account for the methane-DIC conversion in the Lake Kinneret sediments. Also, we observed no or very little ^{13}C-enrichment in the DIC pool following similar incubations with marine sediments, which showed net methanogenesis and contained similar abundance of methane-metabolizing archaea to that of Lake Kinneret sediments based on the detection of *mcrA* with qPCR (Sela-Adler et al., 2015; Amiel, 2018; Vigderovich et al., 2019; Yorshensky, 2019) (Table S6). Therefore, under natural conditions, methanogens alone are unlikely to produce our observed considerable amounts of DIC just by back flux.

4.4 The progression of methane oxidation over time

The geochemical and microbial profiles and fresh sediment incubations show evidence for Fe-AOM in the methanic zone of Lake Kinneret, which removes about 10-15% of the produced methane (Adler et al., 2011; Sivan et al., 2011). Anaerobic archaea appear to carry out methane turnover in these reduced sediments by reverse methanogenesis, but methanotrophic Methylococcales are also involved in methane oxidation. This fits other studies, which show more evidence pointing to the existence of aerobic bacterial activity in the deep anoxic hypolimnion of lakes and in the shallow sediments (Beck et al., 2013; Oswald et al., 2016; Martinez-Cruz et al., 2017; Cabrol et al., 2020). These bacteria live alongside strict methanogenic anaerobes and iron reducers, probably in a complex interaction, which increases the iron reduction in a cryptic cycle that should be further explored.

The presence of aerobes and anaerobes together in nature, even 20 meters below the thermocline and oxycline, means that small amounts of oxygen could be trapped in nano-niches or even in mineral layers (Wang et al., 2018), even if they are not detected by sensitive sensors. This oxygen portion may not be removed by purging the freshly collected sediments at the beginning of our experiments but is rather slowly used by the methanotrophs for their survival. However, after several incubation stages, and intensive purging and prolonged time, only archaea remained active and were involved in methane turnover. It appears that methanotrophic bacteria cannot survive the long-term slurry incubations and thus iron reduction and methane oxidation are decoupled.

To conclude, trace levels of oxygen may fuel aerobic methane oxidizers in a cryptic cycle between oxygen and iron in the natural lake methanic sediments, and they are responsible for part of the methane oxidation and maybe the iron reduction. The rest of the methane is oxidized to DIC by methanogens or ANME-1. The DIC production from methane turnover in the long-term experiments is performed only by methanogens or ANME-1. It seems less likely that this is by back flux alone, but rather by active metabolic AOM by reverse methanogenesis and an external electron acceptor. Sulfate, nitrate, nitrite, and manganese are unlikely. Humic substances are the most likely electron acceptors used with or without the natural iron oxides.

Competing interests. The authors declare that they have no conflict of interest.

https://doi.org/10.5194/bg-2021-223
Preprint. Discussion started: 24 August 2021

Acknowledgements

We would like to thank B. Sulimani and O. Tzabari from the Yigal Allon Kinneret Limnological Laboratory for their onboard technical assistance. We thank all of O. Sivan's lab members for their help during sampling, and especially to N. Lotem for the help with the mass balance calculations and discussions and to E. Eliani-Russak for her technical assistance. Many thanks to K. Hachmann from M. Elvert's lab for his help during lipid analysis and to J. Gropp for insightful discussions on the back flux. This work was supported by the ERC consolidator grant (818450) and the Israel Science Foundation (857-2016) of O. Sivan. Funding for M. Elvert was provided by the Deutsche Forschungsgemeinschaft (DFG) (49926684) and EXC 2077 (390741601). Funding for M. Rubin-Blum was provided by the Israel Science Foundation (913/19), the U.S.-Israel Binational Science Foundation (2019055) and Ministry of Science and Technology (1126), and H. Vigderovich was supported by the student fellowship of the Israeli water authority.

References

Adler, Michal, Eckert, W., & Sivan, O. (2011). Quantifying rates of methanogenesis and methanotrophy in Lake Kinneret sediments (Israel) using pore-water profiles. *Limnology and Oceanography*, *56*(4), 1525–1535. https://doi.org/10.4319/lo.2011.56.4.1525

Aepfler, R. F., Bühring, S. I., & Elvert, M. (2019). Substrate characteristic bacterial fatty acid production based on amino acid assimilation and transformation in marine sediments. *FEMS Microbiology Ecology*, *95*(10), 1–15. https://doi.org/10.1093/femsec/fiz131

Amiel, N. (2018). *Authigenic magnetite in deep sediments Authigenic magnetite in deep sediments*.

Aromokeye, D. A., Kulkarni, A. C., Elvert, M., Wegener, G., Henkel, S., Coffinet, S., Eickhorst,T., Oni, O. E., Richter-Heitmann, T., Schnakenberg, A., Taubner, H., Wunder, L., Yin, X., Zhu, Q., Hinrichs, KU., Kasten, S., & Friedrich, M. W. (2020). Rates and Microbial Players of Iron-Driven Anaerobic Oxidation of Methane in Methanic Marine Sediments. *Frontiers in Microbiology*, *10*(January), 1–19. https://doi.org/10.3389/fmicb.2019.03041

Arshad, A., Speth, D. R., De Graaf, R. M., Op den Camp, H. J. M., Jetten, M. S. M., & Welte, C. U. (2015). A metagenomics-based metabolic model of nitrate-dependent anaerobic oxidation of methane by Methanoperedens-like archaea. *Frontiers in Microbiology*, *6*(DEC), 1–14. https://doi.org/10.3389/fmicb.2015.01423

Bai, Y. N., Wang, X. N., Wu, J., Lu, Y. Z., Fu, L., Zhang, F., Lau, TC., & Zeng, R. J. (2019). Humic substances as electron acceptors for anaerobic oxidation of methane driven by ANME-2d. *Water Research*, *164*, 114935. https://doi.org/10.1016/j.watres.2019.114935

Bankevich, A., Nurk, S., Antipov, D., Gurevich, A. a., Dvorkin, M., Kulikov, A. S., Lesin, V. M., Nicolenko, S. I., Pham, S., Prjibelski, A. D., Sirotkin, A. V., Vyahhi, N., Tesler, G., Aleksyev, A. M., & Pevzner, P. a. (2012). SPAdes: A New Genome Assembly Algorithm and Its Applications to Single-Cell Sequencing.

https://doi.org/10.5194/bg-2021-223
Preprint. Discussion started: 24 August 2021

533 *Journal of Computational Biology*, *19*(5), 455–477. https://doi.org/10.1089/cmb.2012.0021

534 Bar-Or, I., Ben-Dov, E., Kushmaro, A., Eckert, W., & Sivan, O. (2015). *Methane-related changes in*
535 *prokaryotes along geochemical profiles in sediments of Lake Kinneret (Israel) Methane-related changes*
536 *in prokaryotes along geochemical profiles in sediments of Lake Kinneret (Israel)*. (August).
537 https://doi.org/10.5194/bg-12-2847-2015

538 Bar-Or, I., Elvert, M., Eckert, W., Kushmaro, A., Vigderovich, H., Zhu, Q., Ben-Dov, E., & Sivan, O. (2017).
539 Iron-Coupled Anaerobic Oxidation of Methane Performed by a Mixed Bacterial-Archaeal Community
540 Based on Poorly Reactive Minerals. *Environmental Science & Technology*, *51*, 12293–12301.
541 https://doi.org/10.1021/acs.est.7b03126

542 Beal, E. J., House, C. H., & Orphan, V. J. (2009). Manganese-and Iron-Dependent Marine Methane Oxidation.
543 *Science (New York, N.Y.)*, *325*(5937), 184–187. https://doi.org/10.1126/science.1169984

544 Beck, D. A. C., Kalyuzhnaya, M. G., Malfatti, S., Tringe, S. G., del Rio, T. G., Ivanova, N., Lidstorm, M. E., &
545 Chistoserdova, L. (2013). A metagenomic insight into freshwater methane-utilizing communities and
546 evidence for cooperation between the Methylococcaceae and the Methylophilaceae. *PeerJ*, *2013*(1), 1–23.
547 https://doi.org/10.7717/peerj.23

548 Boetius, A., Ravenschlag, K., Schubert, C. J., Rickert, D., Widdel, F., Gieseke, A., Amann, R., Jørgensen, B.B.,
549 Witte, U., & Pfannkuche, O. (2000). A marine microbial consortium apparently mediating AOM. *Nature*,
550 *407*(October), 623–626.

551 Bond, D. R., & Lovley, D. R. (2002). Reduction of Fe(III) oxide by methanogens in the presence and absence of
552 extracellular quinones. *Environmental Microbiology*, *4*(2), 115–124. https://doi.org/10.1046/j.1462-
553 2920.2002.00279.x

554 Bottrell, S. H., Parkes, R. J., Cragg, B. A., & Raiswell, R. (2000): Isotopic evidence for anoxic pyrite oxidation
555 and stimulation of bacterial sulphate reduction in marine sediments, *J. Geol. Soc. London*,157, 711–714.
556 https://doi.org/10.1144/jgs.157.4.711.

557 Cabrol, L., Thalasso, F., Gandois, L., Sepulveda-Jauregui, A., Martinez-Cruz, K., Teisserenc, R., Tananaev, N.,
558 Tveit, A., Svenning, M. M., & Barret, M. (2020). Anaerobic oxidation of methane and associated
559 microbiome in anoxic water of Northwestern Siberian lakes. *Science of the Total Environment*, *736*,
560 139588. https://doi.org/10.1016/j.scitotenv.2020.139588

561 Chuang, P. C., Yang, T. F., Wallmann, K., Matsumoto, R., Hu, C. Y., Chen, H. W., Lin, S., Sun, CH., Li, HC.,
562 Wang, Y., & Dale, A. W. (2019). Carbon isotope exchange during anaerobic oxidation of methane (AOM)
563 in sediments of the northeastern South China Sea. *Geochimica et Cosmochimica Acta*, *246*, 138–155.
564 https://doi.org/10.1016/j.gca.2018.11.003

565 Conrad, R. (2009). The global methane cycle: Recent advances in understanding the microbial processes
566 involved. *Environmental Microbiology Reports*, *1*(5), 285–292. https://doi.org/10.1111/j.1758-
567 2229.2009.00038.x

https://doi.org/10.5194/bg-2021-223
Preprint. Discussion started: 24 August 2021

568 Dershwitz, P., Bandow, N. L., Yang, J., Semrau, J. D., McEllistrem, M. T., Heinze, R. A., Fonseca, M.,
569 Ledesma, J. C., Jennett, J. R., DiSpirito, A. M., Athwal, N. S., Hargrove, M. S., Bobik, T. A., Zischka, H.,
570 & DiSpirito, A. A. (2021). Oxygen Generation via Water Splitting by a Novel Biogenic Metal Ion-
571 Binding Compound. *Applied and Environmental Microbiology*, *87*(14), 1–14.
572 https://doi.org/10.1128/aem.00286-21

573 Eckert, T. (2000). The Influence of Chemical Stratification in the Water Column on Sulfur and Iron Dynamics
574 in Pore Waters and Sediments of Lake Kinneret, Israel. *M.Sc. Thesis*, University of Bayreuth, Germany.

575 Egger, M., Rasigraf, O., Sapart, C. J., Jilbert, T., Jetten, M. S. M., Röckmann, T., van der Veen, C., Bândă, N.,
576 Kartal, B., Ettwig, K. F., & Slomp, C. P. (2015). Iron-mediated anaerobic oxidation of methane in
577 brackish coastal sediments. *Environmental Science and Technology*, *49*(1), 277–283.
578 https://doi.org/10.1021/es503663z

579 Elul, M., Rubin-Blum, M., Ronen, Z., Bar-Or, I., Eckert, W., & Sivan, O. (2021). Metagenomic insights into the
580 metabolism of microbial communities that mediate iron and methane cycling in Lake Kinneret sediments.
581 *Biogeosciences Discussions*, 1–24. https://doi.org/10.5194/bg-2020-329

582 Elvert, M., Boetius, A., Knittel, K., & Jørgensen, B. B. (2003). Characterization of specific membrane fatty
583 acids as chemotaxonomic markers for sulfate-reducing bacteria involved in anaerobic oxidation of
584 methane. *Geomicrobiology Journal*, *20*(4), 403–419. https://doi.org/10.1080/01490450303894

585 Ettwig, Katharina F, Butler, M. K., Le Paslier, D., Pelletier, E., Mangenot, S., Kuypers, M. M. M., Schreiber, F.,
586 Dutilh, B. E., Zedelius, J., de Beer, D. Gloerich, J., Wessels, H. J. C. T., van Alen, T., Luesken, F., Wu,
587 M. L., van de Pas-Schoonen K. T., Op den Camp, H. J. M., Jansen-Megens, E. M., Francojs, KJ.,
588 Stunnenberg, H., Weissenbach, J., Jetten, M. S. M., & Strous, M. (2010). Nitrite-driven anaerobic
589 methane oxidation by oxygenic bacteria. *Nature*, *464*(7288), 543–548.
590 https://doi.org/10.1038/nature08883

591 Fan, L., Dippold, M. A., Ge, T., Wu, J., Thiel, V., Kuzyakov, Y., & Dorodnikov, M. (2020). Anaerobic
592 oxidation of methane in paddy soil: Role of electron acceptors and fertilization in mitigating CH4 fluxes.
593 *Soil Biology and Biochemistry*, *141*, 107685. https://doi.org/10.1016/j.soilbio.2019.107685

594 Glöckner, F. O., Yilmaz, P., Quast, C., Gerken, J., Beccati, A., Ciuprina, A., Bruns, G., Yarza, P., Peplies, J.,
595 Westram, R., & Ludwig, W. (2017). 25 years of serving the community with ribosomal RNA gene
596 reference databases and tools. *Journal of Biotechnology*, *261*(February), 169–176.
597 https://doi.org/10.1016/j.jbiotec.2017.06.1198

598 Gropp, J., Iron, M. A., & Halevy, I. (2021). Theoretical estimates of equilibrium carbon and hydrogen isotope
599 effects in microbial methane production and anaerobic oxidation of methane. *Geochimica et*
600 *Cosmochimica Acta*, *295*, 237–264. https://doi.org/10.1016/j.gca.2020.10.018

601 Gruber-Vodicka, H. R., Seah, B. K., & Pruesse, E. (2019). phyloFlash — Rapid SSU rRNA profiling and
602 targeted assembly from metagenomes. *BioRxiv*, 521922. https://doi.org/10.1101/521922

603 Hadas, O., & Pinkas, R. (1995). Sulphate reduction in the hypolimnion and sediments of Lake Kinneret , Israel.

https://doi.org/10.5194/bg-2021-223
Preprint. Discussion started: 24 August 2021

Freshwater Biology, (33), 63–72.

Hallam, S. J., Putnam, N., Preston, C. M., Detter, J. C., Rokhsar, D., Richardson, P. H., & DeLong, E. F. (2004). Reverse methanogenesis: Testing the hypothesis with environmental genomics. *Science*, *305*(5689), 1457–1462. https://doi.org/10.1126/science.1100025

Haroon, M. F., Hu, S., Shi, Y., Imelfort, M., Keller, J., Hugenholtz, P., Yuan, Z., & Tyson, G. W. (2013). Anaerobic oxidation of methane coupled to nitrate reduction in a novel archaeal lineage. *Nature*, *500*(7464), 567–570. https://doi.org/10.1038/nature12375

He, Q., Yu, L., Li, J., He, D., Cai, X., & Zhou, S. (2019). Electron shuttles enhance anaerobic oxidation of methane coupled to iron(III) reduction. *Science of the Total Environment*, *688*, 664–672. https://doi.org/10.1016/j.scitotenv.2019.06.299

Hoehler, T. M., Alperin, M. J., Albert, D. B., & Martens, C. S. (1994). Field and laboratory, evidence for a methane-sulfate reducer consortium.pdf. *Global Biogeochemical Cycles*, *8*(4), 451–463.

Holler, T., Wegener, G., Niemann, H., Deusner, C., Ferdelman, T. G., Boetius, A., Brunner, B., & Widdel, F. (2011). Carbon and sulfur back flux during anaerobic microbial oxidation of methane and coupled sulfate reduction. *Proceedings of the National Academy of Sciences of the United States of America*, *108*(52). https://doi.org/10.1073/pnas.1106032108

Holmkvist, L., Ferdelman, T. G., & Jørgensen, B. B. (2011). A cryptic sulfur cycle driven by iron in the methane zone of marine sediment (Aarhus Bay, Denmark). *Geochimica et Cosmochimica Acta*, *75*(12), 3581–3599. https://doi.org/10.1016/j.gca.2011.03.033

Kang, D. D., Li, F., Kirton, E., Thomas, A., Egan, R., An, H., & Wang, Z. (2019). MetaBAT 2: An adaptive binning algorithm for robust and efficient genome reconstruction from metagenome assemblies. *PeerJ*, *2019*(7), 1–13. https://doi.org/10.7717/peerj.7359

Kits, K. D., Klotz, M. G., & Stein, L. Y. (2015). Methane oxidation coupled to nitrate reduction under hypoxia by the Gammaproteobacterium Methylomonas denitrificans, sp. nov. type strain FJG1. *Environmental Microbiology*, *17*(9), 3219–3232. https://doi.org/10.1111/1462-2920.12772

Knittel, K., & Boetius, A. (2009). Anaerobic oxidation of methane: Progress with an unknown process. *Annual Review of Microbiology*, *63*, 311–334. https://doi.org/10.1146/annurev.micro.61.080706.093130

Kostka, J. E., Dalton, D. D., Skelton, H., Dollhopf, S., & Stucki, J. W. (2002). Growth of iron (III)-reducing bacteria on clay minerals as the sole electron acceptor and comparison of growth yields on a variety of oxidized iron forms. *Applied and Environmental Microbiology*, *68*(12), 6256–6262. https://doi.org/10.1128/AEM.68.12.6256-6262.2002

Lai, C. Y., Dong, Q. Y., Rittmann, B. E., & Zhao, H. P. (2018). Bioreduction of Antimonate by Anaerobic Methane Oxidation in a Membrane Biofilm Batch Reactor. *Environmental Science and Technology*, *52*(15), 8693–8700. https://doi.org/10.1021/acs.est.8b02035

Li, X., Hou, L., Liu, M., Zheng, Y., Yin, G., Lin, X., Cheng, L., Li, Y., & Hu, X. (2015). Evidence of Nitrogen

639 Loss from Anaerobic Ammonium Oxidation Coupled with Ferric Iron Reduction in an Intertidal Wetland.
640 *Environmental Science and Technology*, *49*(19), 11560–11568. https://doi.org/10.1021/acs.est.5b03419

641 Lin, Y. S., Lipp, J. S., Yoshinaga, M. Y., Lin, S. H., Elvert, M., & Hinrichs, K. U. (2010). Intramolecular stable
642 carbon isotopic analysis of archaeal glycosyl tetraether lipids. *Rapid Communications in Mass*
643 *Spectrometry*, *24*(19), 2817–2826. https://doi.org/10.1002/rcm.4707

644 Liu, D., Dong, H., Bishop, M. E., Zhang, J., Wang, H., Xie, S., Wang, S., huang, L., & Eberl, D. D. (2012).
645 Microbial reduction of structural iron in interstratified illite-smectite minerals by a sulfate-reducing
646 bacterium. *Geobiology*, *10*(2), 150–162. https://doi.org/10.1111/j.1472-4669.2011.00307.x

647 Liu, Deng, Dong Hailiang, H., Bishop, M. E., Wang, H., Agrawal, A., Tritschler, S., Eberl, D. D., & Xie, S.
648 (2011). Reduction of structural Fe(III) in nontronite by methanogen Methanosarcina barkeri. *Geochimica*
649 *et Cosmochimica Acta*, *75*(4), 1057–1071. https://doi.org/10.1016/j.gca.2010.11.009

650 Lovley, D R, Coates, J. D., BluntHarris, E. L., Phillips, E. J. P., & Woodward, J. C. (1996). Humic substances
651 as electron acceptors for microbial respiration. *Nature*, Vol. 382, pp. 445–448.
652 https://doi.org/10.1038/382445a0

653 Lovley, Derek R, & Klug, M. J. (1983). Sulfate Reducers Can Outcompete Methanogens at Concentrations
654 Sulfate Reducers Can Outcompete Methanogens Sulfate Concentrationst at Freshwater. *Applied and*
655 *Environmental Microbiology*, *45*, 187–194.

656 Luo, J. H., Chen, H., Hu, S., Cai, C., Yuan, Z., & Guo, J. (2018). Microbial Selenate Reduction Driven by a
657 Denitrifying Anaerobic Methane Oxidation Biofilm. *Environmental Science and Technology*, *52*(7),
658 4006–4012. https://doi.org/10.1021/acs.est.7b05046

659 Luo, J. H., Wu, M., Yuan, Z., & Guo, J. (2017). Biological Bromate Reduction Driven by Methane in a
660 Membrane Biofilm Reactor. *Environmental Science and Technology Letters*, *4*(12), 562–566.
661 https://doi.org/10.1021/acs.estlett.7b00488

662 Martinez-cruz, K., Leewis, M., Charold, I., Sepulveda-jauregui, A., Walter, K., Thalasso, F., & Beth, M. (2017).
663 Science of the Total Environment Anaerobic oxidation of methane by aerobic methanotrophs in sub-
664 Arctic lake sediments. *Science of the Total Environment*, *607–608*, 23–31.
665 https://doi.org/10.1016/j.scitotenv.2017.06.187

666 Meador, T. B., Gagen, E. J., Loscar, M. E., Goldhammer, T., Yoshinaga, M. Y., Wendt, J., Thomm, M., &
667 Hinrichs, K. U. (2014). Thermococcus kodakarensis modulates its polar membrane lipids and elemental
668 composition according to growth stage and phosphate availability. *Frontiers in Microbiology*, *5*(JAN), 1–
669 13. https://doi.org/10.3389/fmicb.2014.00010

670 Meister, P., Liu, B., Khalili, A., Böttcher, M. E., & Jørgensen, B. B. (2019). Factors controlling the carbon
671 isotope composition of dissolved inorganic carbon and methane in marine porewater: An evaluation by
672 reaction-transport modelling. *Journal of Marine Systems*, *200*(August), 103227.
673 https://doi.org/10.1016/j.jmarsys.2019.103227

https://doi.org/10.5194/bg-2021-223
Preprint. Discussion started: 24 August 2021

674 Meyerdierks, A., Kube, M., Kostadinov, I., Teeling, H., Glöckner, F. O., Reinhardt, R., & Amann, R. (2010).
675 Metagenome and mRNA expression analyses of anaerobic methanotrophic archaea of the ANME-1 group.
676 *Environmental Microbiology*, *12*(2), 422–439. https://doi.org/10.1111/j.1462-2920.2009.02083.x

677 Moran, J. J., House, C. H., Freeman, K. H., & Ferry, J. G. (2005). Trace methane oxidation studied in several
678 Euryarchaeota under diverse conditions. *Archaea*, *1*(5), 303–309. https://doi.org/10.1155/2005/650670

679 Moran, J. J., House, C. H., Thomas, B., & Freeman, K. H. (2007). Products of trace methane oxidation during
680 nonmethyltrophic growth by Methanosarcina. *Journal of Geophysical Research: Biogeosciences*, *112*(2),
681 1–7. https://doi.org/10.1029/2006JG000268

682 Newman, D. K., & Kolter, R. (2000). A role for excreted quinones in extracellular electron transfer. *Nature*,
683 *405*(6782), 94–97.

684 Nollet, L., Demeyer, D., & Verstraete, W. (1997). Effect of 2-bromoethanesulfonic acid and Peptostreptococcus
685 productus ATCC 35244 addition on stimulation of reductive acetogenesis in the ruminal ecosystem by
686 selective inhibition of methanogenesis. *Applied and Environmental Microbiology*, *63*(1), 194–200.
687 https://doi.org/10.1128/aem.63.1.194-200.1997

688 Nurk, S., Bankevich, A., & Antipov, D. (2013). Assembling genomes and mini-metagenomes from highly
689 chimeric reads. *Research in Computational Molecular Biology*, 158–170. https://doi.org/10.1007/978-3-
690 642-37195-0

691 Nüsslein, B., Chin, K. J., Eckert, W., & Conrad, R. (2001). Evidence for anaerobic syntrophic acetate oxidation
692 during methane production in the profundal sediment of subtropical Lake Kinneret (Israel). *Environmental*
693 *Microbiology*, *3*(7), 460–470. https://doi.org/10.1046/j.1462-2920.2001.00215.x

694 Orembland, R. S., & Capone, D. G. (1988). *Use of "Specific" Inhibitors in Biogeochemistry and Microbial*
695 *Ecology* (Vol. 10). https://doi.org/10.2307/4514

696 Orphan, V. J., House, C. H., & Hinrichs, K. U. (2001). Methane-Consuming Archaea Revealed by Directly
697 Coupled Isotopic and Phylogenetic Analysis. *Science*, *293*(July), 484–488.
698 https://doi.org/10.1126/science.1061338

699 Oswald, K., Milucka, J., Brand, A., Hach, P., Littmann, S., Wehrli, B., Albersten, M., Daims, H., Wagner, M.,
700 Kuypers, M. M. M., Schubert, C. J., & Milucka, J. (2016). Aerobic gammaproteobacterial methanotrophs
701 mitigate methane emissions from oxic and anoxic lake waters. *Limnology and Oceanography*, *61*, S101–
702 S118. https://doi.org/10.1002/lno.10312

703 Raghoebarsing, A. A., Pol, A., Van De Pas-Schoonen, K. T., Smolders, A. J. P., Ettwig, K. F., Rijpstra, W. I. C.,
704 Schouten, S., Sinninghe Damsté, J. S., Op den Camp, H. J. M., Jetten, M. S. M., & Strous, M. (2006). A
705 microbial consortium couples anaerobic methane oxidation to denitrification. *Nature*, *440*(7086), 918–
706 921. https://doi.org/10.1038/nature04617

707 Ratasuk, N., & Nanny, M. A. (2007). Characterization and quantification of reversible redox sites in humic
708 substances. *Environmental Science and Technology*, *41*(22), 7844–7850.

https://doi.org/10.1021/es071389u

Reeburgh, W. S. (2007). Oceanic Methane Biogeochemistry. *ChemInform*, *38*(20), 486–513. https://doi.org/10.1002/chin.200720267

Saunois, M., Stavert, A. R., Poulter, B., Bousquet, P., Canadell, J. G., Jackson, R. B., Raymond, P. A., Dlugokencky, E. J., Houweling, S., Patra, P. K., Ciais, P., Arora, V. K., Bastviken, D., Bergamaschi, P., Blake, D. R., Brailsford, G., Bruhwiler, L., Carlson, K. M., Carrol, M., Castaldi, S., Chandra, N., Crevoisier, C., Crill, P. M., Covey, K., Curry, C. L., Etiope, G., Frankenberg, C., Gedney, N., Hegglin, M. I., Höglund-Isaksson, L., Hugelius, G., Ishizawa, M., Ito, A., Janssens-Maenhout, G., Jensen, K. M., Joos, F., Kleinen, T., Krummel, P. B., Langenfelds, R. L., Laruelle, G. G., Liu, L., Machida, T., Maksyutov, S., McDonald, K. C., McNorton, J., Miller, P. A., Melton, J. R., Morino, I., Müller, J., Murguia-Flores, F., Naik, V., Niwa, Y., Noce, S., O'Doherty, S., Parker, R. J., Peng, C., Peng, S., Peters, G. P., Prigent, C., Prinn, R., Ramonet, M., Regnier, P., Riley, W. J., Rosentreter, J. A., Segers, A., Simpson, I. J., Shi, H., Smith, S. J., Steele, L. P., Thornton, B. F., Tian, H., Tohjima, Y., Tubiello, F. N., Tsuruta, A., Viovy, N., Voulgarakis, A., Weber, T. S., van Weele, M., van der Werf, G. R., Weiss, R. F., Worthy, D., Wunch, D., Yin, Y., Yoshida, Y., Zhang, W., Zhang, Z., Zhao, Y., Zheng, B., Zhu, Q., Zhu, Q., and Zhuang, Q.: The Global Methane Budget 2000–2017, Earth Syst. Sci. Data, 12, 1561–1623, https://doi.org/10.5194/essd-12-1561-2020, 2020.

Scheller, S., Yu, H., Chadwick, G. L., & Mcglynn, S. E. (2016). *Artificial electron acceptors decouple archaeal methane oxidation from sulfate reduction*. *351*(6274), 1754–1756.

Scheller, S., Yu, H., Chadwick, G. L., McGlynn, S. E., & Orphan, V. J. (2016). Artificial electron acceptors decouple archaeal methane oxidation from sulfate reduction. *Science*, *351*(6274), 1754–1756. https://doi.org/10.1126/science.aad7154

Scott, D. T., Mcknight, D. M., Blunt-Harris, E. L., Kolesar, S. E., & Lovley, D. R. (1998). Quinone moieties act as electron acceptors in the reduction of humic substances by humics-reducing microorganisms. *Environmental Science and Technology*, *32*(19), 2984–2989. https://doi.org/10.1021/es980272q

Segarra, K. E. a, Comerford, C., Slaughter, J., & Joye, S. B. (2013). Impact of electron acceptor availability on the anaerobic oxidation of methane in coastal freshwater and brackish wetland sediments. *Geochimica et Cosmochimica Acta*, *115*, 15–30. https://doi.org/10.1016/j.gca.2013.03.029

Sela-Adler, M., Herut, B., Bar-Or, I., Antler, G., Eliani-Russak, E., Levy, E., Makovsky, Y., & Sivan, O. (2015). Geochemical evidence for biogenic methane production and consumption in the shallow sediments of the SE Mediterranean shelf (Israel). *Continental Shelf Research*, *101*, 117–124. https://doi.org/10.1016/j.csr.2015.04.001

Serruya, C. (1971). Lake Kinneret: the nutrient chemistry of the Sediments. *Limnology and Oceanography*, *16*(May), 510–521.

Shuai, W., & Jaffé, P. R. (2019). Anaerobic ammonium oxidation coupled to iron reduction in constructed wetland mesocosms. *Science of the Total Environment*, *648*, 984–992.

https://doi.org/10.1016/j.scitotenv.2018.08.189

Sieber, C. M. K., Probst, A. J., Sharrar, A., Thomas, B. C., Hess, M., Tringe, S. G., & Banfield, J. F. (2018). Recovery of genomes from metagenomes via a dereplication, aggregation and scoring strategy. *Nature Microbiology*, *3*(7), 836–843. https://doi.org/10.1038/s41564-018-0171-1

Sivan, O., Adler, M., Pearson, A., Gelman, F., Bar-Or, I., John, S. G., & Eckert, W. (2011). Geochemical evidence for iron-mediated anaerobic oxidation of methane. *Limnology and Oceanography*, *56*(4), 1536–1544.

Stookey, L. L. (1970). Ferrozine-a new spectrophotometric reagent for iron. *Analytical Chemistry*, *42*(7), 779–781. https://doi.org/10.1021/ac60289a016

Sturt, H. F., Summons, R. E., Smith, K., Elvert, M., & Hinrichs, K. U. (2004). Intact polar membrane lipids in prokaryotes and sediments deciphered by high-performance liquid chromatography/electrospray ionization multistage mass spectrometry - New biomarkers for biogeochemistry and microbial ecology. *Rapid Communications in Mass Spectrometry*, *18*(6), 617–628. https://doi.org/10.1002/rcm.1378

Su, G., Zopfi, J., Yao, H., Steinle, L., Niemann, H., & Lehmann, M. F. (2020). Manganese/iron-supported sulfate-dependent anaerobic oxidation of methane by archaea in lake sediments. *Limnology and Oceanography*, *65*(4), 863–875. https://doi.org/10.1002/lno.11354

Tamames, J., & Puente-Sánchez, F. (2019). SqueezeMeta, A Highly Portable, Fully Automatic Metagenomic Analysis Pipeline. *Frontiers in Microbiology*, *9*. https://doi.org/10.3389/fmicb.2018.03349

Timmers, P. H. A., Welte, C. U., Koehorst, J. J., Plugge, C. M., Jetten, M. S. M., & Stams, A. J. M. (2017). Reverse Methanogenesis and Respiration in Methanotrophic Archaea. *Archaea*, *2017*(Figure 1). https://doi.org/10.1155/2017/1654237

Treude, T., Krause, S., Maltby, J., Dale, A. W., Coffin, R., & Hamdan, L. J. (2014). Sulfate reduction and methane oxidation activity below the sulfate-methane transition zone in Alaskan Beaufort Sea continental margin sediments: Implications for deep sulfur cycling. *Geochimica et Cosmochimica Acta*, *144*, 217–237. https://doi.org/10.1016/j.gca.2014.08.018

Treude, T., Niggemann, J., Kallmeyer, J., Wintersteller, P., Schubert, C. J., Boetius, A., & Jørgensen, B. B. (2005). Anaerobic oxidation of methane and sulfate reduction along the Chilean continental margin. *Geochimica et Cosmochimica Acta*, *69*(11), 2767–2779. https://doi.org/10.1016/j.gca.2005.01.002

Valenzuela, E. I., Avendaño, K. A., Balagurusamy, N., Arriaga, S., Nieto-Delgado, C., Thalasso, F., & Cervantes, F. J. (2019). Electron shuttling mediated by humic substances fuels anaerobic methane oxidation and carbon burial in wetland sediments. *Science of the Total Environment*, *650*, 2674–2684. https://doi.org/10.1016/j.scitotenv.2018.09.388

Valenzuela, E. I., & Cervantes, F. J. (2021). The role of humic substances in mitigating greenhouse gases emissions: Current knowledge and research gaps. *Science of the Total Environment*, *750*, 141677. https://doi.org/10.1016/j.scitotenv.2020.141677

780 Valenzuela, E. I., Prieto-Davó, A., López-Lozano, N. E., Hernández-Eligio, A., Vega-Alvarado, L., Juárez, K.,
781 García-González, A. S., López, M. G., & Cervantes, F. J. (2017). Anaerobic methane oxidation driven by
782 microbial reduction of natural organic matter in a tropical wetland. *Applied and Environmental*
783 *Microbiology*, *83*(11), 1–15. https://doi.org/10.1128/AEM.00645-17

784 Vigderovich, H., Liang, L., Herut, B., Wang, F., Wurgaft, E., Rubin-Blum, M., & Sivan, O. (2019). Evidence
785 for microbial iron reduction in the methanogenic sediments of the oligotrophic SE Mediterranean
786 continental shelf. *Biogeosciences Discussions*, 1–25. https://doi.org/10.5194/bg-2019-21

787 Wang, L., Miao, X., Ali, J., Lyu, T., & Pan, G. (2018). Quantification of Oxygen Nanobubbles in Particulate
788 Matters and Potential Applications in Remediation of Anaerobic Environment. *ACS Omega*, *3*(9), 10624–
789 10630. https://doi.org/10.1021/acsomega.8b00784

790 Wang, Y., & Newman, D. K. (2008). Redox Reactions of Phenazine Antibiotics with Ferric (Hydr)oxides and
791 Molecular Oxygen. *Environmental Science & Technology*, *42*(7), 2380–2386.

792 Wang, Z., Guo, F., Liu, L., & Zhang, T. (2014). Evidence of Carbon Fixation Pathway in a Bacterium from
793 Candidate Phylum SBR1093 Revealed with Genomic Analysis. *PLoS ONE*, *9*(10).
794 https://doi.org/10.1371/journal.pone.0109571

795 Wegener, G., Gropp, J., Taubner, H., Halevy, I., & Elvert, M. (2021). Sulfate-dependent reversibility of
796 intracellular reactions explains the opposing isotope effects in the anaerobic oxidation of methane. *Science*
797 *Advances*, *7*(19), 1–14. https://doi.org/10.1126/sciadv.abe4939

798 Wu, Y.-W., Tang, Y.-H., Tringe, S. G., Simmons, B. A., & Singer, S. W. (2014). MaxBin: an automated
799 binning method to recover individual genomes from metagenomes using. *Microbiome*, *2*(26), 4904–4909.
800 Retrieved from https://microbiomejournal.biomedcentral.com/articles/10.1186/2049-2618-2-26

801 Wuebbles, D. J., & Hayhoe, K. (2002). Atmospheric methane and global change. *Earth-Science Reviews*, *57*(3–
802 4), 177–210. https://doi.org/10.1016/S0012-8252(01)00062-9

803 Yorshensky, O. (2019). *Iron Reduction in Deep Marine Sediments of the Eastern Mediterranean Continental*
804 *Shelf and the Yarqon Estuary Iron Reduction in Deep Marine Sediments of the Eastern Mediterranean*
805 *Continental Shelf and the Yarqon Estuary*. Ben Gurion University of the Negev.

806 Yoshinaga, M. Y., Holler, T., Goldhammer, T., Wegener, G., Pohlman, J. W., Brunner, B., Kuypers, M. M. M.,
807 Hinrichs, K. U., & Elvert, M. (2014). Carbon isotope equilibration during sulphate-limited anaerobic
808 oxidation of methane. *Nature Geoscience*, *7*(3), 190–194. https://doi.org/10.1038/ngeo2069

809 Zehnder, a J., & Brock, T. D. (1979). Methane formation and methane oxidation by methanogenic bacteria.
810 *Journal of Bacteriology*, *137*(1), 420–432.

811 Zhang, X., Xia, J., Pu, J., Cai, C., Tyson, G. W., Yuan, Z., & Hu, S. (2019). Biochar-Mediated Anaerobic
812 Oxidation of Methane. *Environmental Science and Technology*, *53*(12), 6660–6668.
813 https://doi.org/10.1021/acs.est.9b01345

814 Zheng, Y., Wang, H., Liu, Y., Zhu, B., Li, J., Yang, Y., Qin, W., Chen, L., Wu, X., Chistoserdova, L., & Zhao,

https://doi.org/10.5194/bg-2021-223
Preprint. Discussion started: 24 August 2021

F. (2020). Methane-Dependent Mineral Reduction by Aerobic Methanotrophs under Hypoxia. *Environmental Science and Technology Letters*, *7*(8), 606–612. https://doi.org/10.1021/acs.estlett.0c00436